# Electronic structure and spectral properties of paramagnetic point defects in Si₃N₄

Gianfranco Pacchioni* and Davide Erbetta

*Istituto Nazionale di Fisica della Materia, Dipartimento di Scienza dei Materiali, Università di Milano-Bicocca,
via Cozzi 53, I-20125 Milano, Italy*

The geometric and electronic structure and the optical, vibrational, and magnetic properties of paramagnetic point defects in $Si_3N_4$ have been studied by means of *ab initio* quantum-chemical methods. Using cluster models and gradient-corrected density functional theory or configuration interaction (CI) wave functions, we have studied the $N_3\equiv Si^\bullet$ and $Si_2=N^\bullet$ paramagnetic point defects, also known as $K^0$ and $N^0$ centers, respectively. The computed ground-state properties, in particular the hyperfine coupling constants of $N_3\equiv Si^\bullet$ and $Si_2=N^\bullet$, the vibrational spectra of the corresponding hydrogenated centers, $N_3\equiv Si$—H and $Si_2=N$—H, and the valence density of states are correctly described, showing the adequacy of the cluster models used for the study of point defects in silicon nitride. The optical transitions associated with $N$ and $K$ centers have been computed by means of CI calculations. The results are compared with those of the analogous defects in $SiO_2$, the nonbridging oxygen and the $E'$ center, respectively. [S0163-1829(99)12741-3]

## I. INTRODUCTION

Amorphous silicon nitride films are widely used in microelectronics as gate dielectrics in thin-film transistors or as charge storage layers in metal-nitride-oxide semiconductor nonvolatile memory devices.[1–18] Usually, the films are prepared by plasma-enhanced chemical vapor deposition at relatively low temperatures. The films obtained in this way contain large concentrations of hydrogen, and the material is thus denoted $a$-$SiN_x$:H, where typically $x < 1.5$. Amorphous silicon nitride, $a$-$Si_3N_4$, and amorphous silicon-nitrogen alloys, $a$-$SiN_x$, can also be prepared by reactive sputtering of silicon in a nitrogen-containing atmosphere. It is believed that the Si dangling bonds, $N_3\equiv Si^\bullet$, also called the $K$ centers, in $a$-$SiN_x$:H thin films are the origin of the memory traps in memory devices and of the charging effects in thin-film transistors.[1,16] The $K$ center has three charge states, $K^+$ ($N_3\equiv Si^+$), $K^0$ ($N_3\equiv Si^\bullet$), and $K^-$ ($N_3\equiv Si^-$). The $K^0$ center is paramagnetic and is observable by electron spin resonance (ESR).[10] The $K^0$ center is metastable, and it has been found that ultraviolet (UV) light converts the charged $K$ centers into $K^0$, while annealing at 200 °C converts the $K^0$ centers back to $K^+$ and $K^-$.[11,12] More recently, another point defect has been identified experimentally in amorphous silicon nitride, the $N$ dangling bond or $N$ center, $Si_2=N^\bullet$.[13] This defect has been observed after thermal treatment at relatively high temperature, $>500$ °C.[13] It has been suggested that this defect is created by hydrogen dissociation from the preexisting N—H centers which transform into $N^+$ and $N^-$ centers, two charged variants of the $N$ center.[16] These diamagnetic precursors are then converted into their paramagnetic state by UV light. The simultaneous presence of $K^0$ and $N^0$ centers has been observed in as-deposited films by irradiating the films by UV at low temperature ($T < 200$ K).[12] Another paramagnetic nitrogen center has been observed under special conditions and attributed to an unpaired electron strongly localized on two inequivalent nitrogen atoms bonded to each other.[12]

Because of the technological importance of silicon nitride, several experimental studies have been dedicated to the nature of the defects present in the material.[3,5,7,10–13,16] Theoretical studies on the electronic structure of this material have also been reported,[1,19–28] but, to the best of our knowledge, no systematic first-principles study of the electronic structure of $K$ and $N$ centers in silicon nitride has been performed so far. Theoretical studies based on simplified Hamiltonians have been reported to describe the relative position of the defect energy levels with respect to the valence- and conduction-band edges.[1,20,21]

In the present study we report high-quality *ab initio* calculations on the geometric and electronic structure of $K$ and $N$ centers. Using cluster models, we have determined the magnetic properties, in particular the hyperfine coupling constants (hfcc's), the vibrational modes (for the hydrogenated Si—H and N—H centers), and the optical transitions of the $N_3\equiv Si^\bullet$ and $Si_2=N^\bullet$ point defects. The results provide a firm basis for the assignment of the observed spectral features to these centers and give additional information on their structure.

## II. COMPUTATIONAL APPROACH

$Si_3N_4$ occurs in two crystalline forms $\alpha$ and $\beta$, containing, respectively, 28 and 14 atoms per unit cell.[29] The bonding is covalent polar, with Si atoms being tetrahedrally coordinated by nitrogen atoms and nitrogen being threefold coordinated in a planar or nearly planar configuration, Fig. 1. Amorphous silicon nitride prepared by chemical vapor deposition (CVD) at high temperatures is essentially stoichiometric and contains very little hydrogen. A continuous random network model of $a$-$Si_3N_4$ built according to these configurations gives a good description of the radial distribution function.[28] We have modeled the point defects in crystalline $Si_3N_4$ by means of cluster models. The broken bonds at the cluster periphery have been saturated by H atoms, a commonly used technique to ''embed'' clusters of semiconducting or insulating materials.[30–32] In some cases no constraint has been introduced in the cluster structure, and the models can be considered as purely molecular. More realistic models have been obtained by cutting the cluster from the periodic structure of
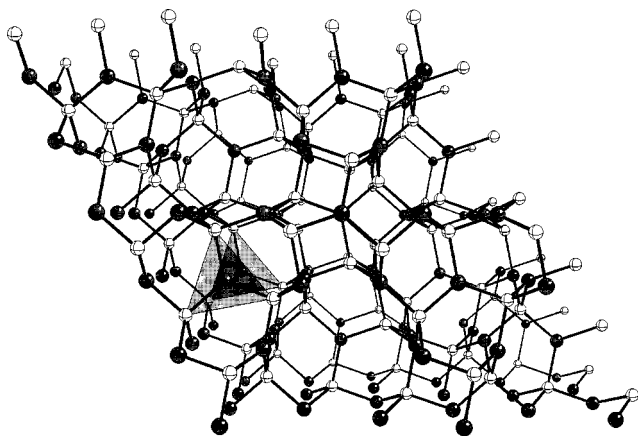
FIG. 1. The structure of crystalline $\alpha$-Si$_3$N$_4$. The planar arrangement of the Si atoms around N is shown.

$\alpha$-Si$_3$N$_4$ and $\beta$-Si$_3$N$_4$ derived from x-ray diffraction data.[29] In this second case the embedding H atoms were fixed at a distance of 1.48 Å from the Si atoms and at 1.01 Å from the N atoms along the Si—N or N—Si directions of Si$_3$N$_4$, respectively. The position of all Si and N atoms of the cluster has been fully optimized. The fixed H atoms provide a simple representation of the mechanical embedding of the solid matrix. Of course, saturation with H atoms does not include the long-range Madelung potential of the crystal. The charges of our atoms determined according to the Mulliken populations are not very large, Si, $+1.3\pm0.2$, and N, $-1.1\pm0.2$, and larger charges have been reported by other authors.[25] This may be a limitation in our models. On the other hand, we have sufficient evidence that clusters saturated with H atoms give accurate results for several observable properties of SiO$_2$,[31–35] a material where the Madelung potential should be of comparable if not of larger importance than in Si$_3$N$_4$. In the following we will specifically comment on those properties which may be affected by the Madelung potential.

The cluster wave functions have been constructed using local Gaussian-type atomic orbitals basis sets. The Si, N, and terminal H atoms have been treated with a 6-31 G basis set.[36] The atoms involved in defect description (e.g., the Si or N atoms of the $K$ and $N$ centers, respectively, and their first neighbors) have been described with a more flexible 6-31G* basis set including also a set of $d$ polarization functions.[37] Even larger basis sets of triple-zeta (TZ) and TZ plus polarization (TZP) quality,[38,39] have been used for the determination of some ground-state properties as discussed below. For the largest models we used a MINI basis set[40] on the Si, N, and H atoms at the cluster border, while the central part where the defect is localized has been treated with 6-31G and 6-31G* basis sets.

Geometry optimizations have been performed at the density functional theory (DFT) level by computing analytical gradients of the total energy. For open-shell systems we performed spin-polarized calculations where two sets of Kohn-Sham orbitals for $\alpha$ and $\beta$ electrons are determined. Ground-state properties have been determined with nonlocal DFT calculations using the hybrid Becke-3 (Ref. 41) and the Lee-Yang-Parr[42] forms of the exchange and correlation functionals, respectively (B3LYP). In this hybrid DFT approach

the Hartree-Fock exchange is partially mixed in with the DFT exchange. Pure DFT calculations using the Becke[43] and the Lee-Yang-Parr[42] exchange-correlation functionals (BLYP), Hartree-Fock and second-order perturbation theory calculations (MP2) have also been performed on selected cases. The molecular models have been computed with $C_s$, $C_{2v}$, and $C_{3v}$ symmetry groups, while clusters derived from the Si$_3$N$_4$ structure have been computed without any symmetry element ($C_1$ symmetry group).

The hyperfine interactions of the electron spin with the nuclear spin of $^{29}$Si and $^{14}$N nuclides have been determined for the paramagnetic centers. The hyperfine interaction is anisotropic and the **A** tensor is composed of two terms. The first one, $a_{\text{iso}}$, is related to the isotropic Fermi contact term and depends on the electron density of an $s$ electron at the nucleus according to

$$a_{\text{iso}} = (8\pi/3)g_N\beta_N g_e\beta|\Psi_s(0)|^2, \tag{1}$$

where $g_N$ and $g_e$ are the nuclear and electronic $g$ factors and $\beta_N$ and $\beta$ are the nuclear and Bohr magnetons. The second term of the **A** tensor is a $3\times3$ matrix **B**, which represents the ''classical'' dipolar interaction between two magnetic (electron and nuclear) moments. Here we have considered only the isotropic part, $a_{\text{iso}}$, of the interaction by means of a spin-polarized DFT approach.

Harmonic normal-mode vibrational frequencies and the corresponding intensities have been determined at the DFT-B3LYP level by means of a full vibrational analysis based on the calculation of analytical first and second derivatives of the total energy; an infinite mass has been associated to the terminal H atoms of the cluster to represent a rigid Si$_3$N$_4$ solid matrix. In this way the coupling of the vibrational modes of the terminal N—H or Si—H units with the rest of the modes is eliminated.

Optical transitions have been determined by performing multireference single- and double-excitation configuration interaction (MRD CI) calculations for the ground and excited states of the clusters.[44,45] Single and double excitations with respect to more than one reference or main configuration ($M$) are generated; in this way, it is possible to include directly higher-excitation classes with respect to the leading configuration in the final CI results. The method makes use of an extrapolation technique; only those configurations with an estimated contribution to the total CI energy larger than a given threshold are included in the secular determinant; the contribution to the final CI energy of the remaining configurations is estimated perturbatively based on an extrapolation technique.[44,45] Twenty-five valence electrons have been correlated for both cluster models of $N$ and $K$ centers, respectively. Typically, a few thousand configurations are directly included in the secular problem, while the number of generated configurations can be $1-10\times10^6$. The reported CI energies are extrapolated to this larger CI space. All configurations contributing more than 0.1% to the final CI wave function are used as main ($M$) configurations. Absorption intensities have been estimated by means of the oscillator strength $f$, using the dipole-length operator as

$$f(\mathbf{r}) = \frac{2}{3}|\langle\psi_{e''}|e\mathbf{r}|\psi_{e'}\rangle|^2\Delta E, \tag{2}$$
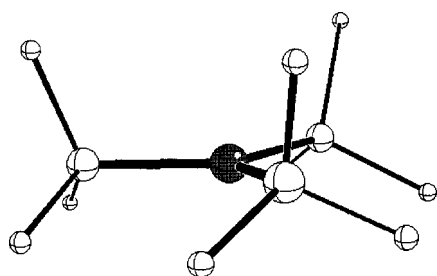
FIG. 2. The optimal structure of the $N(SiH_3)_3$ molecular unit.

where $\Delta E$ is the calculated transition energy. The value of $f$ for a fully allowed transition is of the order of $0.1-1$.

The calculations have been performed with HONDO,[46] GAUSSIAN94,[47] and GAMESS-UK[48] program packages.

## III. RESULTS

### A. Geometrical structure

The bonding of $Si_3N_4$ is best described in terms of interaction of $sp^3$ hybrid orbitals on Si and $sp^2$ hybrids on N to form single Si—N bonds. Since N has five valence electrons, there is a nonbonding lone pair in a $p_z$ orbital of N. This description naturally includes the planarity of the $Si_3\equiv N$ units since this is the usual configuration of $sp^2$ hybrids. However, the reasons for a planar arrangement around N in $Si_3N_4$ has been under discussion for a long time.[1] Two mechanisms have been proposed to account for the planarity of the N site: steric hindrance and $pd\pi$ bonding interaction. The steric hindrance can be explained by the small size of N and by the repulsion among the three —Si$\equiv$ groups bonded to the N atom; this leads to a distortion of the pyramidal structure usually found in N-containing molecular compounds (e.g., $NH_3$). The alternative explanation is based on the role of the $d$ orbitals on Si to form direct $pd\pi$ interactions with the $p_z$ orbital of N which are maximized in case of a planar orientation. Contradicting results about the involvement of the Si $d$ levels in $Si_3N_4$ have been reported in the literature.[1,25] Using various theoretical approaches (Hartree-Fock, MP2, and DFT with two different forms of the exchange correlation functional, BLYP and B3LYP), we have computed the best structure of $N(SiH_3)_3$, Fig. 2, the analogous molecule to $Si_3N_4$, and the isovalent $N(CH_3)_3$ molecule, Table I. The comparison is interesting since the two molecules have different structures in the gas phase, planar and pyramidal, respectively. We also considered two different basis sets, one without $d$ orbitals on N and Si, 6-31G, and one which includes the $d$ orbitals on all atoms, 6-31G*. All methods give the same result, irrespective of the basis set used: $N(CH_3)_3$ is pyramidal, with a C—N—C angle of $113°\pm2°$, while $N(SiH_3)_3$ is planar trigonal, Fig. 2,
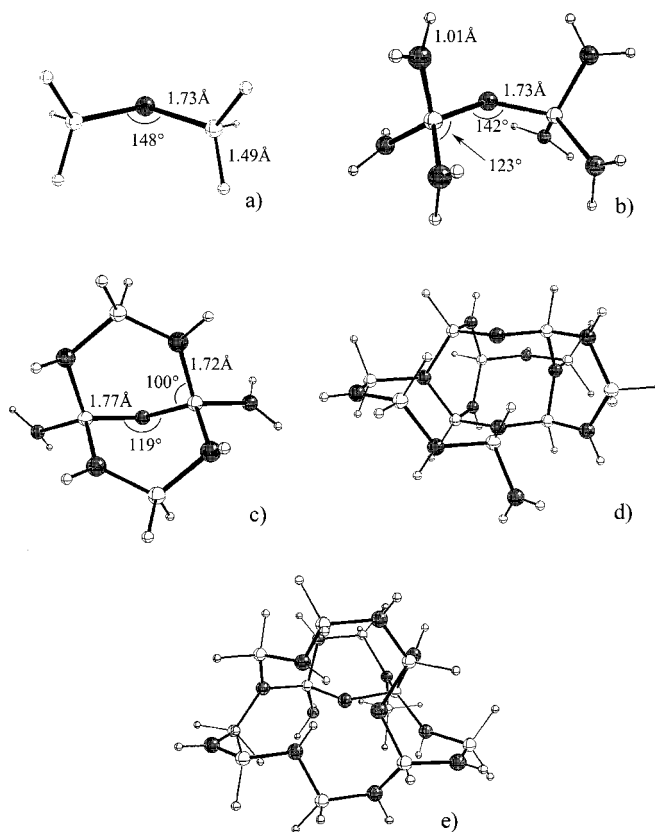


FIG. 3. Cluster models of a $N$ center in $\alpha$-$Si_3N_4$. The first two are molecular models, $(H_3Si)_2N$ (a) and $[(H_2N)_3Si]_2N$ (b), while clusters (c), (d), and (e) are taken from the structure of $Si_3N_4$. For brevity, we denote these clusters as $NSi_2$, $N_7Si_2$, $N_7Si_4$, $N_{12}Si_{10}$, and $N_{14}Si_{12}$. This latter cluster contains two N dangling bonds and has been obtained by removing a Si atom from a nondefective cluster.

in agreement with the experiment. This result is obtained independently of the presence of $d$ functions on Si, showing unambiguously that the reason for the planarity is *not* the $pd\pi$ interaction, but rather the steric hindrance due to the bulky —Si$\equiv$ groups. Of course, any extrapolation of this molecular result to the solid should be done with care, but nevertheless the calculations show that the reasons for planarity are already present at molecular level and are not connected to the involvement of the $d$ orbitals.

Two types of Si-N distances are present in crystalline $\beta$-$Si_3N_4$, 1.72 and 1.76 Å;[29] in a $Si_{13}N_{15}$ cluster model of nondefective $\beta$-$Si_3N_4$ with the H atoms fixed, the optimal distances are $\sim1.75$ and $\sim1.76$ Å, respectively. In amorphous silicon nitride uniform Si-N distances of 1.73 Å have been found from neutron scattering[49] and Monte Carlo simulations.[28] The internal Si—N—Si and N—Si—N angles,

TABLE I. $X$—N—$X$ angle in $N(CH_3)_3$ and $N(SiH_3)_3$ molecules as function of method and basis set.

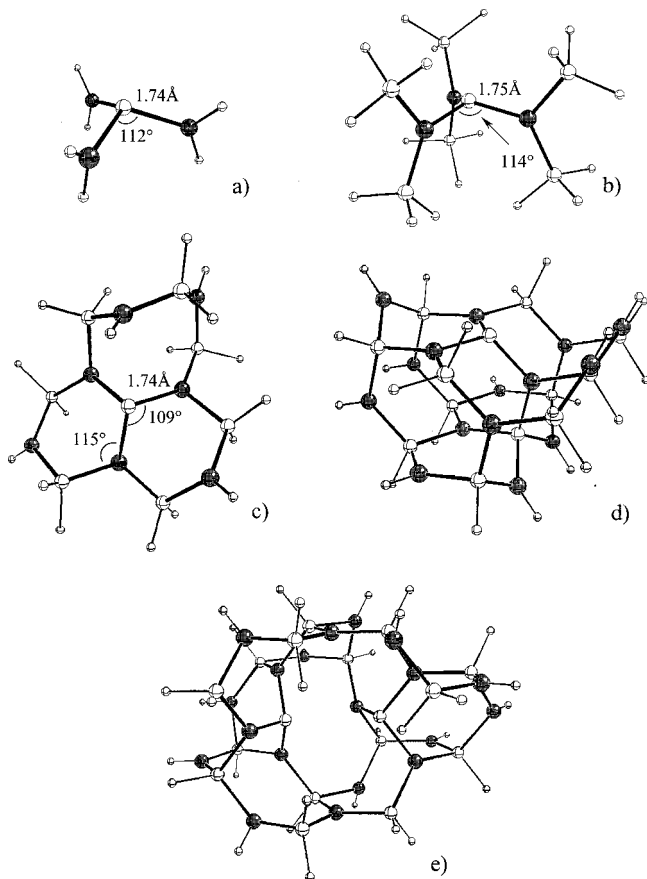| Method | HF | | MP2 | | DFT-BLYP | | DFT-B3LYP | |
|---|---|---|---|---|---|---|---|---|
| Basis set | 6-31G | 6-31G* | 6-31G | 6-31G* | 6-31G | 6-31G* | 6-31G | 6-31G* |
| $N(CH_3)_3$ | 114.2 | 111.9 | 112.3 | 110.4 | 112.8 | 111.4 | 113.3 | 111.5 |
| $N(SiH_3)_3$ | 120.0 | 119.8 | 120.0 | 119.8 | 120.0 | 119.7 | 120.0 | 119.8 |

FIG. 4. Cluster models of a $K$ center in $\alpha$-$Si_3N_4$. The first two are molecular models, $(H_2N)_3Si$ (a) and $[(H_3Si)_2N]_3Si$ (b), while clusters (c), (d), and (e) are taken from the structure of $\alpha$-$Si_3N_4$. For brevity, we denote these clusters as $SiN_3$, $Si_7N_3$, $Si_8N_7$, $Si_{13}N_{15}$, and $Si_{17}N_{19}$. This latter cluster contains two Si dangling bonds and has been obtained by removing a N atom from a non defective cluster.

$120°\pm4°$ and $109°\pm4°$, respectively, are very similar to those of the ideal lattice.

The cluster models used to describe a $N$ center in $Si_3N_4$ are shown in Fig. 3. Some are molecular models, $(H_3Si)_2N$ and $[(H_2N)_3Si]_2N$, Figs. 3(a) and 3(b), while other are taken from the structure of $Si_3N_4$: see Figs. 3(c) and 3(e). For brevity, we denote these clusters as $NSi_2$, $N_7Si_2$, $N_7Si_4$, $N_{12}Si_{10}$, and $N_{14}Si_{12}$, respectively. This latter cluster contains two $N$ centers and has been obtained by removing a Si atom from a model of stoichiometric $Si_3N_4$ and saturating with H atoms two of the resulting N dangling bonds. In the first two cases, $NSi_2$ and $N_7Si_2$, the geometrical optimization has been done without constraint and results in a Si—N—Si bond angle of $145°\pm3°$, Figs. 3(a) and 3(b), while in the

model of the crystal this angle is of 119° only, Fig. 3(c). We will see below that this angle has little effect on properties like the hfcc's. The Si—N distance around the $N$ center is elongated to 1.77 Å. The perturbation on the rest of the cluster due to the presence of a broken bond is negligible and the other distances are close to the bulk values.

In a similar way we used five models of the $K$ center, Fig. 4. The first two, $(H_2N)_3Si$ and $[(H_3Si)_2N]_3Si$, Figs. 4(a) and 4(b), are molecular; the other two are derived from the $Si_3N_4$ lattice, Figs. 4(c)–4(e). The clusters are denoted as $SiN_3$, $Si_7N_3$, $Si_8N_7$, $Si_{13}N_{15}$, and $Si_{17}N_{19}$, respectively. Also, in this case the larger cluster contains two $K$ centers since it has been obtained from a nondefective model by removing a N atom. The geometry optimizations show similar N—Si—N angles for all models; this is a direct consequence of the fact that the tetrahedral coordination around Si is dictated by the formation of $sp^3$ hybrid orbitals, while the Si—N—Si angles are largely dependent on the steric hindrance, hence on the model used. The Si—N distances around the defect are also similar in the four models, 1.74 Å.

### B. Hyperfine coupling constants of $N$ and $K$ centers

The values of the isotropic part of the hfcc's of the unpaired electron with the $^{14}N$ and $^{29}Si$ nuclei in $N$ and $K$ centers are reported in Tables II and III, respectively. The calculations have been performed using the cluster models described in the previous section and two types of basis sets, 6-31G or TZ. In both cases the atom where the unpaired electron is localized and the nearest neighbors are treated with a larger basis including $d$ polarization functions, 6-31G* or TZP. For the $N$ center we found a relatively small constant with $^{14}N$, 15 G (6-31G*) or 6 G (TZP), Table II. Similar values are obtained with the various models considered. Very small hfcc's have been computed for the second-neighbor N atoms in the $N_7Si_4$ model, $\approx3$ G. This shows that the unpaired electron is largely confined on the central N. The experimental value of $a_{iso}$ is $11\pm1$ G,[13] close but not identical to the computed values. The difference between computed and measured values, $\pm5$ G, is due to the basis set and exchange-correlation functional used and not to differences in the local structure of the defect. In fact, the $a_{iso}$ in $Si_2$=$N^\bullet$ is practically insensitive to the geometrical distortions: we have varied the Si—N—Si angle in the $NSi_2$ model, Fig. 2(a), from 90° to 180°, but the changes in $a_{iso}$ are of $\pm3$ G at most. Furthermore, the calculations of the hfcc's for the $N_7Si_4$ model give practically identical results for a geometry taken from the $Si_3N_4$ lattice or after geometrical optimization with the constraint of fixed H atoms. This indi-

TABLE II. Hyperfine coupling constants ($a_{iso}$, in G) of the unpaired electron with $^{14}N$ in cluster models of the $N$ center (DFT-B3LYP results).

| Basis set | $NSi_2$ | $N_7Si_2$ | $N_7Si_4$ | $N_{12}Si_{10}$ | $N_{14}Si_{12}$ | Expt.[a] |
|---|---|---|---|---|---|---|
| 6-31G*/6-31G | 16 | 16 | 15 | 15 | 15 | |
| | | | | | | $11\pm1$ |
| TZP/TZV | 7 | 7 | 6 | | | |

[a]Reference 13.

TABLE III. Hyperfine coupling constants ($a_{iso}$, in G) of the unpaired electron with $^{29}$Si in cluster models of the $K$ center (DFT-B3LYP results).

| Basis set | $SiN_3$ | | $Si_7N_3$ | | $Si_8N_7$ | | $Si_{13}N_{15}$ | | $Si_{17}N_{19}$ | | Expt.[b] | |
| --- | --- | --- | --- | --- | --- | --- | --- | --- | --- | --- | --- | --- |
|  | $^{29}$Si | $^{14}$N | $^{29}$Si | $^{14}$N | $^{29}$Si | $^{14}$N | $^{29}$Si | $^{14}$N | $^{29}$Si | $^{14}$N | $^{29}$Si | $^{14}$N |
| 6-31G*/6-31G | 222 | 8 | 213 | 11 | 273 | 9 | 290 | 8 | 340 | 10 | | |
| | | | | | | | | | | | ~350 | ~4.6 |
| TZP/TZV | 262 | 9 | 237 | 11 | 324 | 9 | | | 395[a] | 10[a] | | |

[a]Single-point calculation on geometry optimized with the 6-31G*/6-31G basis set.
[b]References 7 and 10.

cates that the atomic positions in the optimized cluster are close to those of the crystal, but also that the hfcc is not very sensitive to structural distortions. We cannot exclude, however, that the absence of the Madelung potential in our model is the reason for the small difference found. The small value of $a_{iso}$ is consistent with an unpaired electron wave function of almost pure $2p$ character; the data of spin population analysis show in fact a composition of 4% $2s$ and 96% $2p$ in the singly occupied N orbital. The total spin density on N is of 90%. The small $sp$ hybridization is the reason for the nearly constant value of $a_{iso}$ at various Si—N—Si angles.

Much larger values of $a_{iso}$ are computed for the $K$ center, $N_3\equiv Si^{\cdot}$, Table III. Also the oscillations as function of the model and of the basis set are larger than for the $N$ center. In particular, we observe an increase in $a_{iso}$ when the more flexible TZP basis set is used, but also in correspondence of the $Si_8N_7$ cluster obtained from the $Si_3N_4$ crystal. This result indicates that the hyperfine interactions are much more dependent on the geometrical details than for the $N$ center case. In fact, using the small $SiN_3$ cluster, Fig. 4(a), we observe a rapid increase of $a_{iso}$ by reducing the N—Si—N angle, Fig. 5. A planar $SiN_3$ unit exhibits a very small hfcc, 63 G, which increases to $\approx 250$ G for an angle of 110° (results obtained with the 6-31G* basis set). Thus a more pronounced pyramidal structure of the defect results in a larger hfcc. A similar effect has been recently found for the analogous defect in $a$-$SiO_2$, the $E'$ center.[33] Notice that changes of $\pm 15°$ in the N—Si—N angle imply a relatively small energy cost, Fig. 5. With the best models adopted here, $Si_8N_7$ and $Si_{17}N_{19}$ (2 $K$ centers) and a TZP basis, the $a_{iso}$ is of $360\pm 35$ G, close to the experimental value of 350 G.[10] This large hfcc is indica-

tive of the strong localization of the unpaired electron on Si and of a non-negligible $3s$ character in the unpaired electron wave function. Experimentally, it has been estimated that the wave function has $(55\pm 12)$% of $3p$ and 20% of $3s$ character, with a total contribution from the Si atom of $(75\pm 12)$%.[10] This is different from our calculations, which show a similar contribution of the $3s$ and $3p$ orbitals of Si, $\approx 40$% each, to the unpaired spin wave function. The remaining 20% of the spin density is distributed over the neighbor atoms. Thus, the unpaired electron in the $K$ center appears to be slightly less localized than on the $N$ center, probably because of the larger size of the Si compared to the N atom. The fact that small tails of the unpaired electron wave function extend beyond the Si atom is shown by the small hfcc with the $^{14}$N nuclide measured in electron-nuclear double resonance (ENDOR), 4.6 G, consistent with a spin density of $(1-3)$% on the N atoms bonded to the central Si.[7] Our calculations reproduce this feature quite well giving hfcc's of 7–12 G and a spin density of $(1-5)$% on the N atoms.

Of the four models used to describe the $K$ center, the $Si_7N_3$ molecular structure, Fig. 4(b), gives the least satisfactory results, Table III, with hfcc's which are much too small compared to the experiment. This is due to the particular orientation of the $SiH_3$ groups around the three-coordinated Si. The unpaired electron extends in a region of space with large steric hindrance which causes an artificial polarization of the wave function. We will see below that for the same reason this model does not provide good results for the vibrational modes of a Si—H group. This indicates that the local arrangement of the neighboring groups around the three-coordinated Si is of great importance for the spectral properties of the defect.

### C. Vibrational properties of hydrogenated centers

Hydrogenation of $SiN_x$ alloys tends to replace the Si—Si bonds with Si—H bonds in the silicon-rich alloys and to replace the Si—N bonds with Si—H and N—H bonds in the allows where $x$ is larger. These groups are therefore quite abundant in $a$-$SiN_x$:H materials. On the other hand, even in pure and stoichiometric $Si_3N_4$ the interaction with molecular hydrogen can lead to the following reactions involving the paramagnetic $N^0$ and $K^0$ centers:
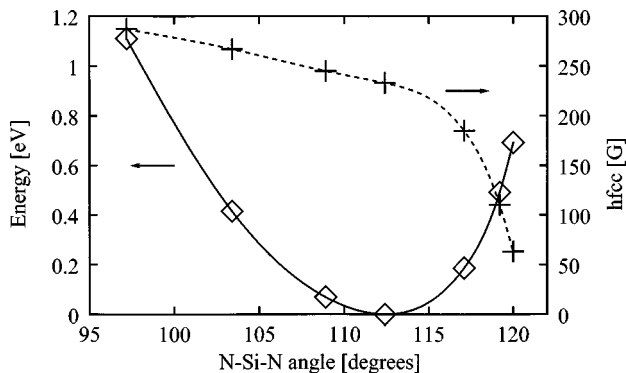


FIG. 5. Dependence on the N-Si-N angle of the hyperfine coupling constant, hfcc, of the unpaired electron with $^{29}$Si in $(NH_2)_3$Si (dotted line); the energy change connected to the angle variation is also shown (solid line).

$$2Si_2\!=\!N^{\cdot}+H_2\rightarrow 2Si_2\!=\!N\!-\!H, \qquad (3)$$

$$2N_3\!\equiv\!Si^{\cdot}+H_2\rightarrow 2N_3\!\equiv\!Si\!-\!H. \qquad (4)$$

TABLE IV. Harmonic frequencies of the N-H bond in the hydrogenated $N$ center.

| | $r_e$(N-H) (Å) | $D_e$(N-H) (eV) | $\omega_e$(N-H) (cm$^{-1}$) | I (km/mol) |
|---|---|---|---|---|
| $NH_3$ | 1.019 | 4.78 | 3571[a] | |
| $NSi_2$ | 1.017 | 4.76 | 3546 | 22.5 |
| $N_7Si_2$ | 1.021 | 4.30 | 3483 | 9.6 |
| $N_7Si_4$ | 1.012 | 4.92 | 3612 | 30.1 |
| Expt.[b] | | | 3335 | |

[a]Experimental values for gas-phase $NH_3$: 3577 cm$^{-1}$ (harmonic), 3444 cm$^{-1}$ (anharmonic).
[b]Reference 2.

A fingerprint of the presence of Si—H or N—H groups in a solid is given by their typical vibrational absorption bands around 3335 and 2200 cm$^{-1}$, respectively.[2]

A hydrogen atom has been attached to the N or Si atom of the cluster where the unpaired electron is localized and the geometry has been repotimized. The results, Tables IV and V, indicate a distance of $1.01 \pm 0.1$ Å for N—H and of $1.48 \pm 0.005$ Å for Si—H. The energy required to dissociate the N—H and Si—H bonds to form the $N^0$ and $K^0$ centers and atomic hydrogen is of the order of $4.8 \pm 0.1$ eV for N—H and $4.2 \pm 0.2$ eV for Si—H. In both cases the homolitic dissociation of the bond requires high energies and is expected to occur only at high temperatures. Since the computed $H_2$ band dissociation energy is of 4.76 eV, reactions (3) and (4) are highly exothermic.

A full vibrational analysis has been performed for the various models of hydrogenated $N$ and $K$ centers; for comparison, the vibrations of the gas-phase $NH_3$ and $SiH_4$ molecules have also been considered, Tables IV and V. The calculation of the vibrations has been done using the harmonic approximation. The $\omega_e$(N—H) is of 3612 cm$^{-1}$ in the $N_7Si_4$ model. Smaller values of $\omega_e$ have been computed for the $NSi_2$ and $N_7Si_2$ molecular models; this latter model, however, is inadequate because of the particular orientation of the $NH_2$ groups and of the resulting steric hindrance with the N—H unit, Fig. 3(b). In fact, the $N_7Si_2$ molecular model gives also a bond distance and a dissociation energy different from that of the other clusters, Table IV. The computed $\omega_e$(N—H), 3612 cm$^{-1}$, is much larger than the values reported for this kind of defect in $Si_3N_4$, 3320–3335 cm$^{-1}$.[2,8] The reason for the discrepancy, however, is not the inaccuracy of the model, but the anharmonicity in the potential. In fact, a large error is found between computed and measured

TABLE V. Harmonic frequencies of the Si-H bond in hydrogenated $K$ center.

| | $r_e$(Si-H) (Å) | $D_e$(Si-H) (eV) | $\omega_e$(Si-H) (cm$^{-1}$) | I (km/mol) |
|---|---|---|---|---|
| $SiH_4$ | 1.487 | 4.11 | 2265 | |
| $SiN_3$ | 1.484 | 4.41 | 2269 | 163 |
| $Si_4N_3$ | 1.487 | 4.32 | 2249 | 209 |
| $Si_7N_3$ | 1.488 | 4.25 | 2432 | 38 |
| $Si_8N_7$ | 1.483 | 4.04 | 2237 | 164 |
| Expt.[a] | | | 2250 | |

[a]Reference 8.

N—H stretching frequency of $NH_3$, Table IV. However, when anharmonic effects are taken into account the two values are nearly identical, Table IV. Anharmonic effects on the N—H bonding in $Si_3N_4$ are expected to be of the same order of magnitude as in the free molecule.

Anharmonic effects are much less important in Si—H vibrations. Here the computed values are of about 2250 cm$^{-1}$, with the only exception of the $Si_7N_3$ cluster where the coupling between the Si—H group and the neighboring $SiH_3$ units leads to a large, unphysical, blueshift of the frequency, Table V. Apart from this particular case, which does not properly represent the structure of the solid, for the rest the computed $\omega_e$(Si—H) is similar in $SiH_4$ or in the $Si_8N_7$ hydrogenated cluster, indicating that the coupling of the Si—H vibrational mode with those of the neighboring atoms is negligible. Experimentally, a broad band around 2180 cm$^{-1}$ has been attributed to Si—H bonds and decomposed into two subbands near 2170 and 2250 cm$^{-1}$ assigned to $(SiN_2)\equiv$Si—H and $N_3\equiv$Si—H units.[8] With a $SiN_2Si$ cluster where a $=$N- unit has been replaced by a $\equiv$Si- group, we found a frequency for the SiH stretching at 2248 cm$^{-1}$, redshifted with respect to the $SiN_3$ cluster by 21 cm$^{-1}$. While the separation with respect to $N_3\equiv$Si—H, 21 cm$^{-1}$, is much smaller than in the experiment, 80 cm$^{-1}$, the assignment of the low-frequency band to a $(SiN_2)\equiv$Si—H group is supported by the calculation.

### D. Band gap and valence-band structure

The optical band gap in unhydrogenated and stoichiometric $Si_3N_4$ is of 5.3 eV according to optical absorption data.[50] In principle, cluster calculations are not adequate to determine gap energies because of the lack of periodic boundary conditions. Nevertheless, it is possible to estimate the size of the gap from a cluster calculation in two independent ways. The results provide an additional test of the adequacy of the cluster model. The first one requires a many-body treatment of both ground and excited states in order to compute the lowest electronic transition of a cluster with all bonds saturated. Here we performed MRD CI calculations on two small models, $N(SiH_3)_3$ and $Si(NH_2)_4$, and we found that in both cases the lowest transition (a singlet-triplet excitation from the highest occupied level, corresponding to the nonbonding N $2p$ level, to the lowest empty Si—N antibonding state) occurs around $6.2 \pm 0.1$ eV. This is only $\approx 10\%$ higher than the experimental gap. The difference, more than to the computational model adopted, has to be attributed to the small size of the cluster used hence to the inaccurate representation of the valence and of the conduction bands. The second way to estimate the band gap is from the analysis of the highest-occupied molecular orbit and lowest-unoccupied molecular orbit (HOMO-LUMO) separation as derived from one-electron orbital energies. It is well known that one-electron energies do not provide a good approximation of an excited state problem like the determination of the optical gap. In particular, Hartree-Fock (HF) calculations largely overestimate the HOMO-LUMO gap (by a factor of 2 easily), while DFT approaches underestimate it. Using a series of relatively large cluster models of nondefective crystalline $Si_3N_4$, we obtain a HOMO-LUMO gap of $7.1 \pm 0.3$ eV. This gap is overestimated with respect to the experimental one by
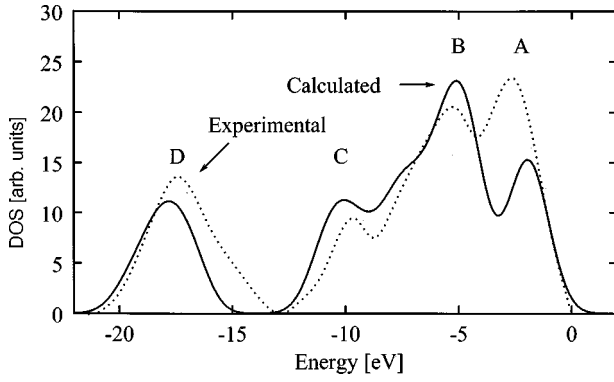
FIG. 6. Valence density of states computed from a $N_{14}S_{13}$ model of nondefective $\alpha$-$Si_3N_4$. The DOS has been obtained by Gaussian broadening (0.75 eV) of the one-electron spectrum. The experimental valence DOS from photoemission experiments is reported for comparison. Intensities [in arbitrary units (a.u.)] have been normalized to the most intense peak. See also Table VI.

about 30%; it is much smaller than one would obtain in HF, but larger than in a pure DFT calculation. The reason is the use of an hybrid DFT approach (B3LYP) where the HF exchange is partially mixed in with the DFT exchange.

The same approach can be used to determine the valence density of states (DOS) by convolution with Gaussian functions of the one-electron energy spectrum. The theoretical spectrum, reported together with the experimental one obtained from x-ray photoemission spectroscopy (XPS) measurements,[51,52] Fig. 6, shows four main features indicated with letters $A-D$ and is qualitatively similar to previously reported DOS curves from first principles[25] and parametrized calculations.[26,27] The position of each peak is compared with data from the literature in Table VI. The valence-band DOS is characterized by a deep feature at $-17.8$ eV (D) due to N $2s$ states and by an upper valence band 12.5 eV wide with three characteristic peaks at $-2.0$ (A), $-5.1$ (B), and $-10.1$ (C) eV. With respect to the experimental spectrum the computed one shows very similar positions of the peaks, while the intensities are not properly reproduced. This is because our clusters are saturated by H bonds that introduce a number of N—H and Si—H features in the valence band. The Si—H bond gives rise to filled states at $\approx -4$ eV, while the N—H bonds contribute to states

TABLE VI. Comparison of calculated and experimental band positions in $Si_3N_4$ (in eV).

| | Calculated this work | Calculated [a] | Expt. [b] |
|---|---|---|---|
| Peak A | $-2.0$ | $-1.2$ | $-2.2$ |
| Peak B | $-5.1$ | $-6.0$ | $-4.8$ |
| Peak C | $-10.1$ | $-11.4$ | $-9.6$ |
| Peak D | $-17.8$ | $-17.2$ | $-17.6$ |
| Band gap | 7.1 (6.1)[c] | 5.3 | 5.3 |
| Valence-band width | 12.5 | 12.5 | 11.4 |
| $K^0$ | 2.2 | 3.1 | 2.5 |

[a]Reference 1.
[b]References 50–52.
[c]From MRD CI calculations; see text.

TABLE VII. Optical transitions of a $N$ center ($=N\bullet$) from MRD CI calculations.[a]

| State | Character[b] | $T_e$ (eV) | $f(r)$ | $\Sigma_i c_i^2$ |
|---|---|---|---|---|
| $X1\ ^2B_1$ | $N_c(2p_x)^1$ | | | 0.95 |
| $1\ ^2A_1$ | $N_c(2p_z)^2 \rightarrow N_c(2p_x)^1$ | 0.7 | $2 \times 10^{-4}$ | 0.96 |
| $1\ ^2A_2$ | $N_l(2p)^2 \rightarrow N_c(2p_x)^1$ | 4.4 | 0.01 | 0.90 |
| $2\ ^2B_1$ | $N_l(2p)^2 \rightarrow N_c(2p_x)^1$ | 4.6 | 0.01 | 0.90 |
| $1\ ^2B_2$ | $[N_l(2p)+N_c(2p_y)]^2 \rightarrow N_c(2p_x)^1$ | 4.6 | $4 \times 10^{-4}$ | 0.92 |
| $2\ ^2B_2$ | $N_l(2p)^2 \rightarrow N_c(2p_x)^1$ | 5.2 | $6 \times 10^{-3}$ | 0.90 |
| $2\ ^2A_1$ | $N_l(2p)^2 \rightarrow N_c(2p_x)^1$ | 5.3 | 0.04 | 0.89 |

[a]$T_e$ = transition energy; $f(r)$ = oscillator strength; $\Sigma_i c_i^2$ = sum of coefficients of all main configurations in the final CI wave function. Calculations based on the N-$Si_2$ model, Fig. 3(b).
[b]$N_c$ = central N atom; $N_l$ = lateral N atoms.

around $\approx -12$ eV.[8] In this respect our models are more representative of hydrogenated than of pure $Si_3N_4$. However, the overall agreement with experiment[51,52] and previous calculations[25,26,27] is very satisfactory and shows that the valence DOS is well described even by relatively small clusters.

It is quite interesting to analyze the position of the singly occupied one-electron levels associated to $N$ and $K$ centers in $Si_3N_4$ as derived from cluster calculations. We found that, irrespective of the cluster size and shape, $N$ centers exhibit a singly occupied level which is close to the top of the valence band formed by the nonbonding N $2p$ levels; in particular, the various clusters considered place this level about 0.8 $\pm 0.1$ eV below the valence-band edge, Table VI (this is due to the spin polarized approach used). On the contrary, the singly occupied level of the $K$ center is well in the gap and gives rise to an impurity state which, according to our calculations, is about 2.2 eV above the top of the valence band, Table VI. These results are in qualitative agreement with the band-structure calculations of Robertson based on a simplified Hamiltonian.[1,53] In these calculations it was found that the $N$ center introduces an occupied state in resonance with the valence band, while the $K$ center is associated to a state just above the midgap, at 3.1 eV from the valence band. The position derived from our calculations is actually in better agreement with the experiment of Iqbal *et al.*[51] The bias electron-spin-resonance (ESR) studies of Jousse *et al.*[54] found a similar position. In any case, the cluster calculations give the same qualitative picture of a periodic approach, further showing the localized nature of these defects and the validity of the cluster model.

### E. Optical transitions

Accurate calculations where correlation effects are explicitly included are possible for a solid only for localized states as those associated to a point defect. Examples of these calculations for diamagnetic and paramagnetic defects in $SiO_2$ have been reported recently.[31–35] The study of the optical transitions of the $K$ and $N$ centers can provide information on the nature, position, and intensity of the corresponding absorption bands. To this end we have performed MRD CI calculations on the neutral $N$ and $K$ centers. Because of the

TABLE VIII. Optical transitions of a $K$ center ($\equiv$Si•) from MRD CI calculations.[a]

| State | Character | $T_e$ (eV) | $f(r)$ | $\Sigma_i c_i^2$ |
|---|---|---|---|---|
| $X1 \; ^2A_1$ | $Si(sp^3)^1$ | | | 0.91 |
| $1 \; ^2A_2$ | $N(2p)^2 \rightarrow Si(sp^3)^1$ | 4.1 | 0.0013 | 0.87 |
| $2 \; ^2A_2$ | $N(2p)^2 \rightarrow Si(sp^3)^1$ | 4.4 | 0.006 | 0.87 |
| $2 \; ^2A_1$ | $N(2p)^2 \rightarrow Si(sp^3)^1$ | 4.9 | 0.009 | 0.86 |
| $3 \; ^2A_1$ | $Si(sp^3)^1 \rightarrow$N-Si antibonding | 5.1 | 0.11 | 0.89 |

[a]$T_e$ = transition energy; $f(r)$ = oscillator strength; $\Sigma_i c_i^2$ = sum of coefficients of all main configurations in the final CI wave function. Calculations based on the $SiN_3$ model, Fig. 4(a).

large size of the CI calculations, we have used small cluster models, $N_7Si_2$, Fig. 3(b), and $SiN_3$, Fig. 4(a), in $C_{2v}$ and $C_s$ symmetries, respectively.

The first excited state of a N dangling bond is found at 0.7 eV above the ground state and corresponds to the local excitation from the doubly occupied $2p_z$ level on $N$ to the singly occupied $2p_x$ level on the same center. Not surprisingly, this $2p$-to-$2p$ transition has very little intensity, $f = 2 \times 10^{-4}$, Table VII. The following excitations involve the $2p$ levels of the neighboring N atoms and the singly occupied $2p$ orbital on the central one. We found a series of transitions of this type in a range between 4.4 and 5.3 eV, Table VII. The intensity of these transitions is larger than for the state at 0.7 eV, but still relatively low. The calculations have been repeated also with a larger basis set including diffuse $s$ and $p$ functions on the central N atom, but the $T_e$ values do not change significantly. Attempts to calculate the first excitation of the unpaired electron into the unoccupied states (conduction band) failed because too many excited states exist below this one. This is an indirect proof of the fact that the N dangling bond lies close to the valence band and that there are no empty states in the gap where the electron can be excited. The weak transitions from the nonbonding $2p$ orbitals of the neighboring N atoms and the singly occupied $2p$ orbital on the central one occur in a range of the spectrum just below the conduction band edge. It is interesting to compare the electronic excitations in $Si_2$=N• with those of the analogous center in $SiO_2$, the nonbridging oxygen (NBO) or $\equiv$Si-O•. Experimentally, a band at 2 eV with relatively low intensity ($f = 10^{-4}$) has been associated to this center.[55] In a recent CI calculation[32] we found for this system a $2p$-to-$2p$ transition at 0.1 eV from the ground state with almost no intensity, and a second band with $T_e = 2.2$ eV and $f(r) \approx 10^{-4}$; this second state is in excellent agreement with the experiment. We have repeated the CI calculation on the transitions of the NBO center is $SiO_2$ using exactly the same method and basis set used here for the $N$ center in $Si_3N_4$. To this end we used a $(HO)_3Si$—$O^•$ cluster with a $C_s$ symmetry plane (in our previous calculations[32] no symmetry elements were present). The results confirm the existence of a low-lying state, at 0.3 eV, followed by a second transition at 2.0 eV (exactly the experimental value) due to an excitation from the nonbonding $2p$ levels on the O neighbors to the singly occupied $2p$ orbital of the NBO. This result provides indirect support to the analysis of the transitions computed for the $N$ center since exactly the same procedure and clusters of similar size have been used.

The transitions of a $K$ center have been studied with the $SiN_3$ cluster model in $C_s$ symmetry, Table VIII. The lowest transitions involve the excitation of one electron form a nonbonding $2p$ orbital on the neighboring N atoms to the singly occupied level on Si; this state is found at 4.1 eV above the ground state; other transitions with similar character are found at slightly higher energies, 4.4 and 4.9 eV, just below the conduction-band edge. The lowest transitions of the $K$ center correspond therefore to a charge transfer from neighboring N atoms to Si; in this case, the difference in the crystalline potential between sites could play a role and affect the transition energies. The first excitation of the unpaired electron into the conduction band is computed at 5.1 eV, Table VIII. This value is probably overestimated because of the inaccurate representation of the conduction band. It is possible that the excitation of the Si dangling bond electron into the conduction band is the origin of the photobleaching of paramagnetic centers in $Si_3N_4$.[16] The electron promoted in the conduction band can then be trapped at a N dangling bond with formation of a $K^+$-$N^-$ pair. A comparison of the transitions of the $K$ defect with the analogous center in silica, the $E'$ center, is useful. The $E'$ center consists of a Si dangling bond bonded to three O atoms.[56] This is the simplest description of the defect and corresponds to what is actually present on the surface of silica.[34,57] In the bulk, however, the structure of the defect is more complex and the nature of the lowest transition is different, involving two Si atoms around the defect.[34] For the surface case, however, the situation can be directly compared. It has been found that the lowest excitation of an isolated $O_3\equiv Si^•$ defect occurs around 6 eV and is due to the promotion of one electron from the nonbridging oxygens to the Si dangling bond;[34] this is practically the same kind of excitation found in $N_3\equiv Si^•$, Table VIII. The main difference is that in the nitride case the excitation occurs at smaller energies, consistent with the smaller gap of this material compared to $SiO_2$.

## IV. CONCLUSIONS

The electronic structure of paramagnetic $N$ and $K$ centers in $Si_3N_4$ has been studied by means of *ab initio* calculations and cluster models. The calculated spectral properties, in particular the isotropic hyperfine coupling constants, the vibrational frequencies of the hydrogenated variants of the $N$ and $K$ centers, and the valence-band density of states are fully consistent with the corresponding measured quantities. This provides a validation of the cluster model approach and additional support to the structural models of $N$ and $K$ centers proposed in the literature.[1,10,13] These point defects consist of an unpaired electron largely localized on a two-coordinated N and on a three-coordinated Si atom, respectively. The two defects give rise to different states; the $N$ center corresponds to a level in the valence band, while the $K$ center is associated to a state placed in the middle of the gap. The position of these levels is important to understand the complex behavior of these centers which tend to disproportionate to $N^+$ and $N^-$ and $K^+$ and $K^-$, respectively.[11,12] Work is in progress to analyze this behavior in more detail.[58]

We also considered the optical transitions associated to these defects. We have found that $N$ centers give rise to weak absorptions in a region from 4.4 up to 5.3 eV, i.e., close to

the conduction-band edge. The $K$ center originates transitions in a similar spectral region. Direct experimental evidence of the transitions described in the calculations does not seem to exist. This may be due to the difficult detection of these weak transitions which could be covered by the tails of the conduction-band edge, but also to the fact these centers are metastable and tend to transform into their charged counterparts. Indeed, photobleaching of $N^0$ centers has been observed for a wide range of photon energies, with maximum efficiency around 2.85 eV.[16] The photobleaching is probably connected to the conversion of neutral $K^0$ and $N^0$ centers

into their charged variants, $K^+$ and $N^-$, through mechanisms which are not yet fully understood.

It has been suggested that the $N$ and $K$ centers are the analogous defects of the NBO and $E'$ centers in silica. We found that there is a close resemblance of the nature of the transitions of a $K$ center in $Si_3N_4$ and an $E'$ center at the surface of $SiO_2$. The main difference is that all the transitions in $Si_3N_4$ are redshifted by about 2 eV, a fact which is consistent with the lower band gap of this material with respect to $SiO_2$. The $N$ center, on the contrary, exhibits transitions which are much higher than in a NBO center in $SiO_2$, despite the fact that the nature of the excitation is similar.

*Electronic address: Gianfranco.Pacchioni@mater.unimib.it

[1] J. Robertson, Philos. Mag. B **63**, 47 (1991).

[2] D. V. Tsu, G. Lucovsky, and M. J. Mantini, Phys. Rev. B **33**, 7069 (1986).

[3] P. A. Pundur, J. G. Shavalgin, and V. A. Gritsenko, Phys. Status Solidi A **94**, K107 (1986).

[4] V. V. Vasilev, I. P. Mikhailovskii, and K. K. Svitashev, Phys. Status Solidi A **95**, K37 (1986).

[5] D. T. Krick and P. M. Lenahan, Phys. Rev. B **38**, 8226 (1988).

[6] L. Yang, B. Abeles, W. Eberhardt, and H. Stasiewski, Phys. Rev. B **39**, 3801 (1989).

[7] W. L. Warren and P. M. Lenahan, Phys. Rev. B **42**, 1773 (1990).

[8] Z. Yin and F. W. Smith, Phys. Rev. B **42**, 3666 (1990).

[9] M. M. Guraya, H. Ascolani, G. Zampieri, J. I. Cisneros, J. H. Dias da Silva, and M. P. Cantão, Phys. Rev. B **42**, 5677 (1990).

[10] P. M. Lenahan and S. E. Curry, Appl. Phys. Lett. **56**, 157 (1990).

[11] W. L. Warren, J. Kanicki, F. C. Rong, and E. H. Poindexter, J. Electrochem. Soc. **139**, 880 (1992).

[12] W. L. Warren, J. Robertson, and J. Kanicki, Appl. Phys. Lett. **63**, 2685 (1993).

[13] W. L. Warren, P. M. Lenahan, and S. E. Curry, Phys. Rev. Lett. **65**, 207 (1990).

[14] D. Chen, J. M. Viner, and P. C. Taylor, Phys. Rev. B **49**, 13 420 (1994).

[15] H. Fritzsche, Appl. Phys. Lett. **65**, 2824 (1994).

[16] W. L. Warren, C. H. Seager, J. Robertson, and E. H. Poindexter, J. Electrochem. Soc. **143**, 3685 (1996).

[17] G. V. Gadiyak, V. G. Gadiyak, M. L. Kosinova, and E. G. Salman, Appl. Surf. Sci. **113/114**, 647 (1997).

[18] H. Ono, T. Ikarashi, Y. Miura, E. Hasegawa, K. Ando, and T. Kitano, Appl. Phys. Lett. **74**, 203 (1999).

[19] J. A. Tossell and G. V. Bibbs, Acta Crystallogr., Sect. A: Cryst. Phys., Diffr., Theor. Gen. Crystallogr. **34**, 463 (1978).

[20] J. Robertson and M. J. Powell, Appl. Phys. Lett. **44**, 415 (1984).

[21] L. Martin-Moreno, E. Martinez, J. A. Vergés, and F. Yndurain, Phys. Rev. B **35**, 9683 (1987).

[22] A. Y. Liu and M. L. Cohen, Phys. Rev. B **41**, 10 727 (1990).

[23] N. Ishii and T. Shimitzu, Phys. Rev. B **48**, 14 653 (1993).

[24] C. Cunha, S. Canuto, and A. Fazzio, Phys. Rev. B **48**, 17 806 (1993).

[25] Yong-Nian Xu and W. Y. Ching, Phys. Rev. B **51**, 17 379 (1995).

[26] V. A. Gritsenko, Yu. N. Morokov, and Yu. N. Novikov, Appl. Surf. Sci. **113/114**, 417 (1997).

[27] V. A. Gritsenko, Yu. N. Morokov, and Yu. N. Novikov, Phys. Solid State **39** (8), 1191 (1997).

[28] F. de Brito Mota, J. F. Justo, and A. Fazzio, Phys. Rev. B **58**, 8323 (1998).

[29] S. N. Ruddlesden and P. Popper, Acta Crystallogr. **11**, 465 (1958).

[30] J. Sauer, P. Ugliengo, E. Garrone, and V. R. Saunders, Chem. Rev. **94**, 2095 (1994).

[31] G. Pacchioni and G. Ieranò, Phys. Rev. Lett. **79**, 753 (1997).

[32] G. Pacchioni and G. Ieranò, Phys. Rev. B **57**, 818 (1998).

[33] G. Pacchioni and M. Vitiello, Phys. Rev. B **58**, 7745 (1998).

[34] G. Pacchioni, G. Ieranò, and A. M. Marquez, Phys. Rev. Lett. **81**, 377 (1998).

[35] G. Pacchioni and R. Ferrario, Phys. Rev. B **58**, 6090 (1998).

[36] W. J. Here, R. Ditchfield, and J. A. Pople, J. Chem. Phys. **56**, 2257 (1972).

[37] G. A. Petersson and M. A. Al-Laham, J. Chem. Phys. **94**, 6081 (1991).

[38] T. H. Dunning, J. Chem. Phys. **55**, 716 (1971).

[39] A. D. McLean and G. S. Chandler, J. Chem. Phys. **72**, 5639 (1980).

[40] H. Tatewaki and S. Huzinaga, J. Chem. Phys. **71**, 4339 (1979).

[41] A. D. Becke, J. Chem. Phys. **98**, 5648 (1993).

[42] C. Lee, W. Yang, and R. G. Parr, Phys. Rev. B **37**, 785 (1988).

[43] A. D. Becke, Phys. Rev. A **38**, 3098 (1988).

[44] R. J. Buenker and S. D. Peyerimhoff, Theor. Chim. Acta **35**, 33 (1974).

[45] R. J. Buenker, S. D. Peyerimhoff, and W. Butscher, Mol. Phys. **35**, 771 (1978).

[46] M. Dupuis, F. Johnston, and A. Marquez, computer program HONDO 8.5 for CHEMStation (IBM Co., Kingston, 1994).

[47] M. J. Frisch *et al.*, computer program GAUSSIAN 94 (Gaussian Inc., Pittsburgh, PA, 1997).

[48] M. F. Guest and P. Sherwood, GAMESS-UK *Reference Manual* (SERC, Daresbury Laboratory, Daresbury, 1992).

[49] M. Misawa, T. Fukunaga, K. Nihara, T. Hirai, and K. Suzuki, J. Non-Cryst. Solids **34**, 313 (1979).

[50] H. R. Phillip, J. Electrochem. Soc. **120**, 295 (1973).

[51] A. Iqbal, W. B. Jackson, C. C. Tsai, J. W. Allen, and C. W. Bates, J. Appl. Phys. **61**, 2947 (1987).

[52] L. Yang, B. Abeles, W. Eberhardt, H. Stasiewski, and D. Sondericker, Phys. Rev. B **39**, 3801 (1989).

[53] J. Robertson, Philos. Mag. B **69**, 307 (1994).

[54] D. Jousse, J. Kanicki, and J. H. Stathis, Appl. Phys. Lett. **54**, 1043 (1989).

[55] L. Skuja, J. Non-Cryst. Solids **179**, 51 (1994).

[56] J. K. Rudra and W. B. Fowler, Phys. Rev. B **35**, 8223 (1987).

[57] V. A. Radzig, Chem. Phys. Rep. **14**, 1206 (1995).

[58] G. Pacchioni and D. Erbetta (unpublished).